JOURNAL OF MATERIALS SCIENCE 21 (1986) 123–130

Sample rocking and rotation in ion beam etching

M. A. TAGG, R. SMITH, J. M. WALLS*
Loughborough University of Technology, Ashby Road, Loughborough, Leicestershire LE11 3TU, UK

Low energy ion bombardment is an established technique for the cleaning, processing and analysis of the surfaces of solids, yet the ion bombardment of these materials does not always produce a flat uniform surface required for many applications. A variety of ion-induced topographies are frequently observed. Rocking and rotation of the sample can reduce unwanted topography by averaging out the angle of incidence effect which is an important factor in the production of surface artefacts. This paper presents a theory which enables a simulation of the development of surfaces in two and three dimensions under the conditions of changes in the surface-beam orientation. It is shown how the discontinuities in surface gradient which occur with inert gas ion bombardment of static samples and are manifested by cones, pyramids and facets can be suppressed by sample rotations and some computer simulations are presented to illustrate this effect.

1. Introduction

Low energy ion bombardment of surfaces is an increasingly important technique in both industrial and scientific environments. It is used, for example, in the production of small scale electronic devices and in surface analysis. However, inert gas ion bombardment of solids can produce well-defined surface features such as pits and pyramids [1]. For many applications this ion-induced topography is an unwanted feature since, for example, it can distort composition–depth profiles in surface analysis or produce pattern distortion if ion etching has been used in the micromachining of electronic devices.

The nucleation of topography can be attributed to a variety of mechanisms such as subsurface defects, initial surface irregularities, material impurities, and effects of implanted gases. This initial topography is further modified during etching since the erosion rate at each point on the surface is a sensitive function of ion-incidence angle.

In earlier work Sykes *et al.* [2] and Makh *et al.* [3] have considered the effect of using two static ion beams in order to minimize unwanted surface topography. Sykes *et al.* [2] have reported experimental evidence that the depth resolution of composition–depth profiles using Auger electron spectroscopy can be improved by using two static ion guns each aligned symmetrically about the sample normal and delivering the same current. A theoretical analysis of the development of surface topography using two ion beams has been carried out by Makh *et al.* [3], who verify that the use of two guns suppresses cone formation and leads to the development of flatter-topped structures.

In principle a better way of averaging the angle of incidence effects would be by rotation of the sample so that it subtends all angles of incidence to the ion beam. This has not always been possible in many UHV systems but with the steady advance of UHV design, sample platforms that have the facility for rotation are becoming more widespread, although in surface analysis of small areas this technique is unlikely to be practical. The purpose of this paper is to develop a theory that will explain the development of topography due to sample rotation in two and three dimensions.

Development of surface topographical features such as etch pits, wave-like structures and conical protuberances as a result of ion bombardment are widely reported in the literature. Whitton *et al.* [4] have investigated the development of cones and associated features on copper. Both Gvosdover *et al.* [5] and Auciello and Kelly [6, 7] have presented results on the evolution of pyramidal structures on surfaces bombarded at normal and oblique incidence angles. More recently Cong-Xin *et al.* [8] have published a detailed paper which systematically studies the influences of ion beam incident angle, energy, dose and target rotation on a variety of substrates. The experimental work in surface topography has been complemented by a number of theoretical studies, and this has been the subject of a comprehensive review by Carter *et al.* [9]. This includes the early work of Stewart and Thompson [10] on the motion of intersecting semi-infinite planes, by Barber *et al.* [11] who used a graphical method based on a slowness erosion curve, and by Carter *et al.* [12] who considered the differential motion of points on a two-dimensional surface.

More recently, other authors have considered these problems, Smith and Walls [13] treated the bombarded surface as a moving wave, and subsequently

**Present address*: VG Scientific Ltd, Imberhorne Lane, East Grinstead, Sussex, UK.

0022–2461/86 $03.00 + .12

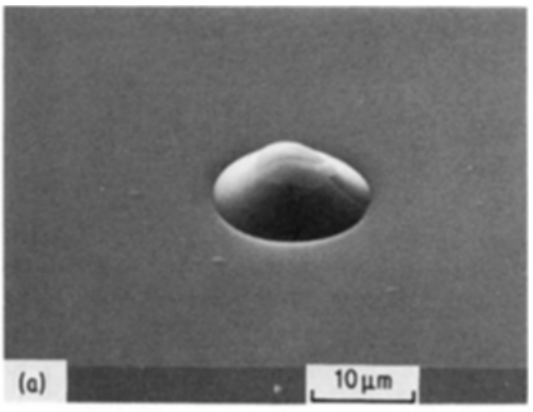

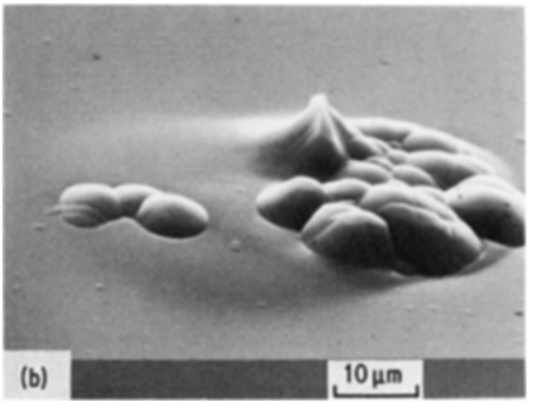

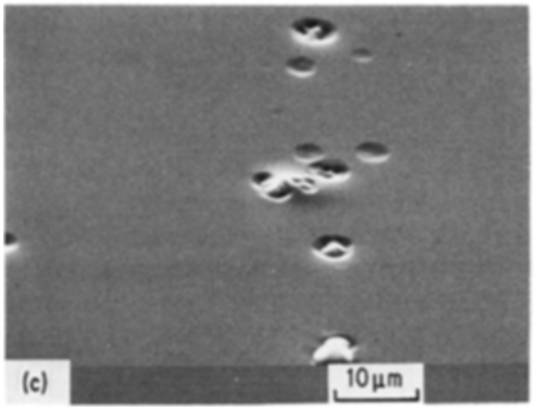

Figure 1 Features observed on AT cut and cerirouge polished quartz crystal platelets. Using sample rotation, the platelets were etched until 11 μm had been removed. Ion beam incidence angles are (a) 20° (b) 20° and (c) 10°.

developed a general three-dimensional theory of surface development. This approach has later been extended to include the effects of ion reflection, [14], redeposition [15], and now in this paper to sample rocking and rotation. The problem of sample rocking and rotation has been considered by other authors, for example, Neureuther *et al.* [16] have proposed a string segment algorithm which accounts for sample rotation, shadowing and faceting, however this is essentially a two-dimensional approach and thus the full effects of rotation can not be fully realized. Cong-Xin *et al.* [8] in a recent paper proposed a mechanism for hillock formation under sample rotation. Similarly Carter *et al.* [17] have considered the problem of ion beams incident on moving substrates but have not carried out any simulations of the development of surface topography.

In this paper, general equations are derived to predict the development of surface shape during ion bombardment under conditions of a time-dependent surface–beam orientation which is used to model sample rotation in the absence of beam shadowing by surface structures. In principle the effect of beam shadowing can also be considered but this would lead to excessive computer time and programme complexity and will therefore only be considered qualitatively. As in previous applications, the theory is developed using the method of characteristics which lends itself fairly conveniently to computer simulation.

2. Experimental details

Ion beam thinning is well suited to the preparation of samples for electron microscopy or surface analysis. It has many advantages over traditional chemical etching such as freedom from chemical contamination and also viability for a wide range of materials. One use that has developed is the tuning of quartz crystal resonators. Since the resonant frequency of quartz crystal is primarily a function of thickness, it is possible by ion beam etching to achieve operating frequencies of 200 MHz or more. The ideal final surface layer of these quartz crystal platelets would be free of crystalline defects and would also be flat. This would ensure loss-free and scatter-free reflection of the acoustic wave. However, ion beam etching can produce unwanted surface topography which can seriously degrade the performance of these resonators. In an attempt to suppress surface features samples could be rotated during etching.

Using a Millitron IBM machine with an argon ion source, several samples at varying ion incidence angles were milled. The sample platform revolves once per minute, and in this time approximately 0.03 μm of the sample are removed. Fig. 1 shows features observed on quartz platelets after 11 μm of the surface has been etched away. Figs. 1a and b, in which the ion gun subtends an angle of 20° to the surface normal, show round hillock features which are probably instigated by buried impurities or surface damage originating from earlier stages of mechanical lapping and polishing. Rotation of the sample has produced these rounded features which are in preference to the sharp cones and pyramids frequently observed without rotation. Fig. 1c in which the ion gun subtends a slightly lower angle of 10° to the surface normal show round crater like features, occasionally with a hillock appearing at the bottom of one of these pits. Essentially, therefore round as opposed to sharp features are produced by rotation of the sample during etching. The computer simulations produced later in this paper verify this conclusion. They show that sample rotation can smooth out initial surface defect whereas static samples will produce cones and pyramids.

3. General theory

Consider a surface whose equation at time t is given by $A(\mathbf{r}, t) = 0$, where $\mathbf{r}$ is the position vector of a point on the surface. Let the surface be subjected to an ion bombardment of uniform incident ion flux ϕ

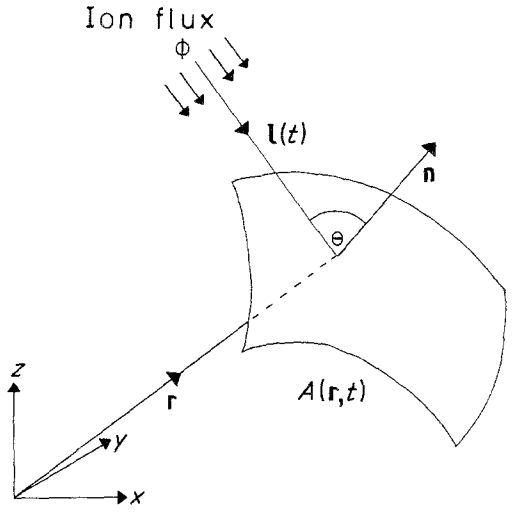

Figure 2 A schematic diagram illustrating the evolution of surface topography during etching.

(ions $cm^{-2} sec^{-1}$) in a direction specified by the unit vector $\mathbf{l} = \mathbf{l}(t)$. Denote the atomic density of the bombarded material by N. Thus the rate of erosion of the target in the surface normal direction is $-\phi/N S \mathbf{l}\cdot\mathbf{n}$, where $\mathbf{n}$ is the unit normal to the surface, and S is the sputtering yield. It is assumed that S is dependent only on the angle between the unit normal and the ion beam direction.

Let $\mathbf{l}\cdot\mathbf{n} = +\cos\theta$, hence the differential equation describing erosion is:

$$\frac{\partial r_n}{\partial t} = \frac{-\phi}{N} S(\theta)\cos\theta \tag{1}$$

where r_n is distance in the normal direction. The geometry is illustrated in a schematic diagram, Fig. 2.

If the equation of the surface is given by

$$0 = A(\mathbf{r}, t) = t - \sigma(\mathbf{r}) \tag{2}$$

then Equation 1 can be written as

$$1 - \frac{\phi}{N} S(\theta)\cos\theta(\sigma_x^2 + \sigma_y^2 + \sigma_z^2)^{1/2} = 0 \tag{3}$$

(see Smith and Walls [13]) and since $\nabla A = -(\sigma_x, \sigma_y, \sigma_z)$

then

$$\mathbf{n} = \frac{-(\sigma_x, \sigma_y, \sigma_z)}{(\sigma_x^2 + \sigma_y^2 + \sigma_z^2)^{1/2}} \tag{4}$$

Hence,

$$\cos\theta = -\frac{(l_1\sigma_x + l_2\sigma_y + l_3\sigma_z)}{(\sigma_x^2 + \sigma_y^2 + \sigma_z^2)^{1/2}} \tag{5}$$

substituting into Equation 3 yields the equation

$$1 + \frac{\phi}{N} S(\theta)(l_1\sigma_x + l_2\sigma_y + l_3\sigma_z) = 0 \tag{6}$$

This equation is now of a suitable form to apply the method of characteristics described by Whitham [18]. Essentially this reduces the partial differential Equation 6 to a set of simultaneous ordinary differential equations. The Hamiltonian H for this system is defined as

$$H = 1 + \frac{\phi}{N} S(\theta)(l_1\sigma_x + l_2\sigma_y + l_3\sigma_z) = 0 \tag{7}$$

Substituting the appropriate Hamiltonian for this system gives the following set of ordinary differential equations describing the motion of a point (x, y, z) on the initial surface.

$$\frac{dx}{dt} = \frac{\phi}{N}[A(l_1 + B\sigma_x) - S(\theta)l_1]$$

$$\frac{dy}{dt} = \frac{\phi}{N}[A(l_2 + B\sigma_y) - S(\theta)l_2]$$

$$\frac{dz}{dt} = \frac{\phi}{N}[A(l_3 + B\sigma_z) - S(\theta)l_3] \tag{8}$$

$$\frac{d\sigma_x}{dt} = C\sigma_x, \quad \frac{d\sigma_y}{dt} = C\sigma_y, \quad \frac{d\sigma_z}{dt} = C\sigma_z$$

where

$$A = \frac{S'(\theta)\cos\theta}{\sin\theta}, \tag{9}$$

$$B = \frac{\cos\theta}{(\sigma_x^2 + \sigma_y^2 + \sigma_z^2)^{1/2}}; \tag{10}$$

$$C = (\dot{l}_1\sigma_x + \dot{l}_2\sigma_y + \dot{l}_3\sigma_z)\left[S(\theta)\frac{-S'(\theta)\cos\theta}{\sin\theta}\right] \tag{11}$$

$$S'(\theta) = \frac{dS(\theta)}{d\theta}, \quad \dot{l}_i = \frac{dl_i(t)}{dt}, \quad i = 1, 2, 3.$$

The essential difference between the above equations and those used to simulate static beams is the appearance of the $\dot{l}_i$ terms on the right hand side of the equations. This means that if the beam direction changes, σ_x, σ_y and σ_z are not constant along the characteristics. Thus the characteristics are not straight lines and a full solution to the problem involves the solution of the six simultaneous ordinary differential Equations 8 for a network of points defining the initial surface.

4. Computer simulation

The set of simultaneous ordinary differential equations derived in the previous section, predict the development of a three-dimensional surface during ion bombardment, the method used to produce practical simulations of this process is now explained. First a digital representation of the initial surface is prescribed, this was achieved in two ways. Contours of constant height (z), defined in the surface, were selected and then a number of points (x, y) corresponding to each height calculated for the appropriate parametric equations. Alternatively a regular grid of points (x, y) covering the surface is computed and the surface height (z) found at each of those points. Having defined the surface, the unit normal $\mathbf{n}_i$ at each initial point (x_i, y_i, z_i) is then computed, this allows θ_i, the angle between the initial ion beam direction and the unit normal to be found. Finally initial values of the vector $(\sigma_x, \chi_y, \sigma_z)$ are required. This is accomplished by noting that at time $t = 0$, $(\sigma_x, \sigma_y, \sigma_z)$

is in the same direction as $\mathbf{n}_i$. This combined with Equation 6 of the previous section, specifies the value of $(\sigma_x, \sigma_y, \sigma_z)$.

Having obtained initial values for the differential equations, these can then be solved, for a suitable timestep t_1, by a computer program. This produces an envelope of points (x_i', y_i', z_i') describing the surface. Originally values on a contoured system corresponding to 7000 data points were used to define the surface, this was found to be the minimum number of points required to produce acceptable computer simulations. This required the solution of 7000 sets of six differential equations, with the consequence that standard computer packages could not be used without incurring a large CPU time. Subsequently a Fortran code based on a Runge Kutta Merson fifth order method [19] was written specifically to solve these equations. The codes uses the specialized nature of the equations and also their symmetry in order to minimize the function evaluations. The advantages in using the Merson method is that error estimates are available, these were checked to ensure errors were within a suitable tolerance. A typical run for 7000 points is about 40 min on the Honeywell Multics system, although this time does depend to a large extent on the rocking and rotation rates and also the timestep. Two-dimensional simulations were also calculated, and essentially the method of solution is identical with the one just described, the system now reducing to a set of four differential equations by omitting one spatial co-ordinate.

In both the two-dimensional and three-dimensional simulations it is possible to obtain physically unrealistic solutions caused by the characteristic lines crossing. The physical explanation of this is that the surface has formed an edge (discontinuity in gradient) and the characteristic method produces a multivalued solution and cannot be applied after such nonlinear wave interactions. It is essential to remove these spurious points since they are unrealistic, and graphical techniques are employed to achieve this. Finally Gino F, Ginosurf and Nag plotting routines are used to produce the final graphical simulations.

5. Results and discussion

5.1. Two-dimensional simulations

For the two-dimensional simulations a sinusoidal profile represented by 201 points was taken as the initial surface shape. The variation of sputtering yield with ion incidence angle was chosen to be the same as used previously for simulating surface erosion by two static ion beams [3] and represents the yield curve for amorphous silicon. The procedure described in the previous section was then carried out for equal timesteps and for a variety of rocking rates β and maximum rocking angles α. For the sake of a systematic study, the direction cosines of the ion beam at time t are chosen to be $[\sin(\alpha\cos\beta t), \cos(\alpha\cos\beta t)]$ i.e. the ion beam orientation is varying between $\pm\alpha$ in simple harmonic motion of frequency β. In practice however such manipulations of the sample are more likely to be carried out manually and in a discrete manner. The results obtained are shown in Fig. 3 which show the successively eroded contours and the characteristic lines for each simulation. As a reference Fig. 3a shows the erosion of the profile for a normal incidence ion beam and no rocking, i.e. $\alpha = 0, \beta = 0$. It can be seen that an edge is formed at the top of the hummock corresponding to a discontinuity, by the third timestep. This edge then persists throughout the remaining period. Figs. 3b, c and d then show the effects of increasing the maximum rocking angle, whilst keeping the rocking rate constant at 2π. Again in Fig. 3b for $\alpha = \pi/12$, an edge has formed by the third timestep, but the discontinuity in surface gradient is much less then in Fig. 3a, and the edge then appears to "open out" on the next timestep, due to the rocking motion. In Fig. 3c and d for $\alpha = \pi/6$, this "opening out" of the edge is more clearly visible and the characteristics do not cross, resulting in a smoother eroded profile. Figs. 3e and g show the effects of increasing the rocking rate β whilst keeping the rocking angle α constant at $\pi/12$. Fig. 3e shows that for a relatively slow rocking rate the top of the profile at any instant tends to point in the direction of the ion beam. Again an edge has formed by the third timestep, but the feature is not as sharp as Fig. 3a. In Fig. 3f for the higher rocking rate the initial surface shape is preserved due to the averaging effect of the rocking motion. Finally in Fig. 3g the high rocking rate has caused the characteristics to become almost straight lines, yet the lines have a spread of orientations very much less than the characteristics for erosion without rocking. The same effect would be achieved if a static beam were incident on a much flatter surface and in comparison to Fig. 3a, the initial surface profile is better preserved.

The simulations described above have only been made for values of α up to $\pi/4$ since rates greater than this would cause various parts of the chosen initial profile to be shadowed requiring extra refinements to the computer programs. In addition, the practical case of the simulation of the erosion of impurities of a different sputtering yield on a surface (possibly responsible in the first instance for the formation of the surface protrusion) has not been carried out. These modifications are currently the subject of further work to enable a larger range of simulations to be made.

5.2. Three-dimensions

In these simulations an exponential hummock is used as a three-dimensional illustration of the technique. The hummock is defined by the equation

$$z = \exp[-(x^2 + y^2)] \qquad (12)$$

with the x–y plane chosen so that the hummock appears to lie on a flat plane. To illustrate the effects of rotation various combinations of the parameters $l_1(t)$, $l_2(t)$, $l_3(t)$, the direction cosines of the ion beam at time t, were taken. The general form of the parameters chosen for the model problem is

$$l_1(t) = \sin(\alpha)\sin(2\pi\beta t)$$

$$l_2(t) = \sin(\alpha)\cos(2\pi\beta t)$$

$$l_3(t) = \cos(\alpha)$$

With these parameters the ion beam describes cones of

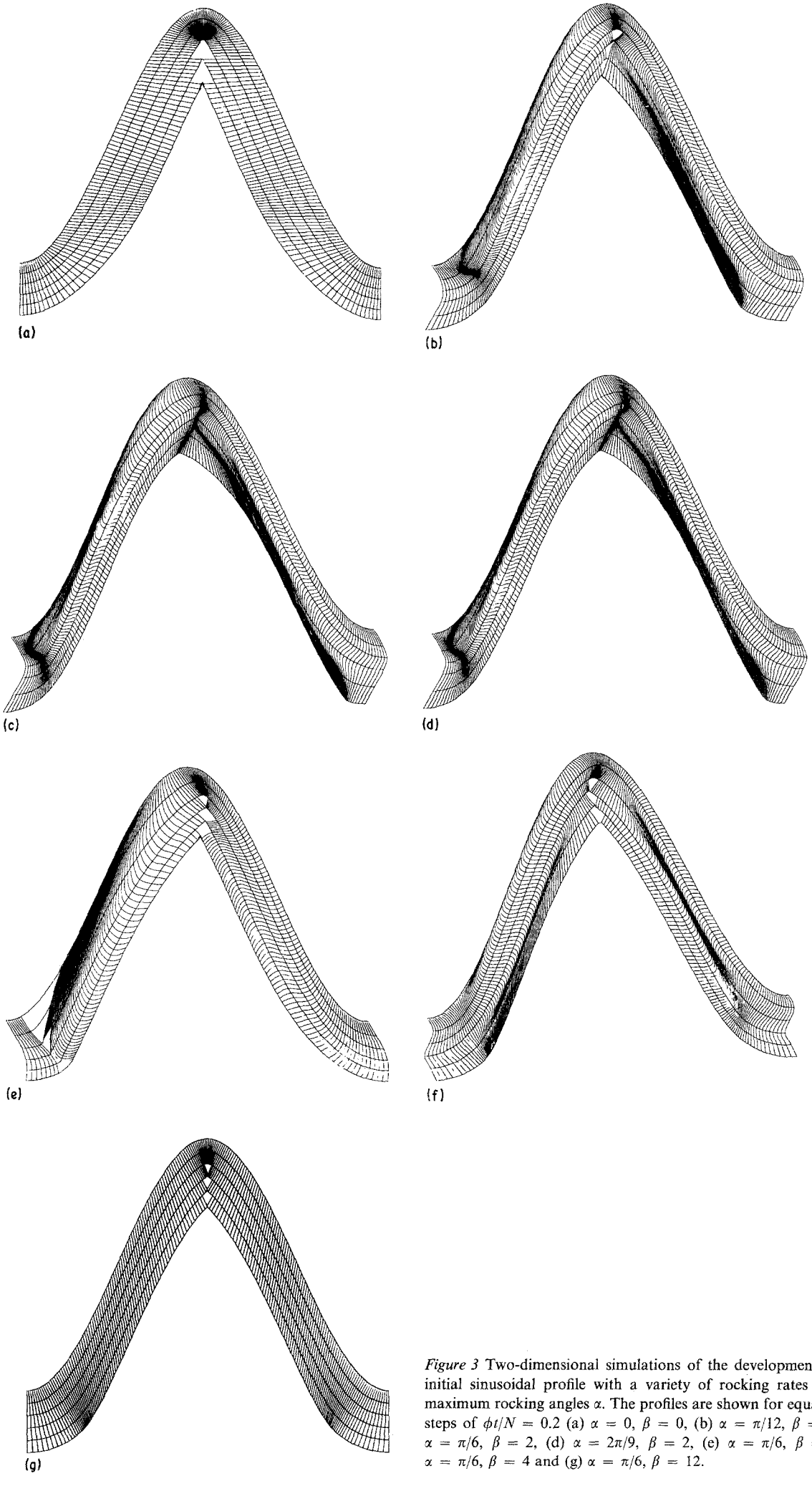

Figure 3 Two-dimensional simulations of the development of an initial sinusoidal profile with a variety of rocking rates β, and maximum rocking angles α. The profiles are shown for equal time-steps of $\phi t/N = 0.2$ (a) $\alpha = 0$, $\beta = 0$, (b) $\alpha = \pi/12$, $\beta = 2$, (c) $\alpha = \pi/6$, $\beta = 2$, (d) $\alpha = 2\pi/9$, $\beta = 2$, (e) $\alpha = \pi/6$, $\beta = 1$ (f) $\alpha = \pi/6$, $\beta = 4$ and (g) $\alpha = \pi/6$, $\beta = 12$.

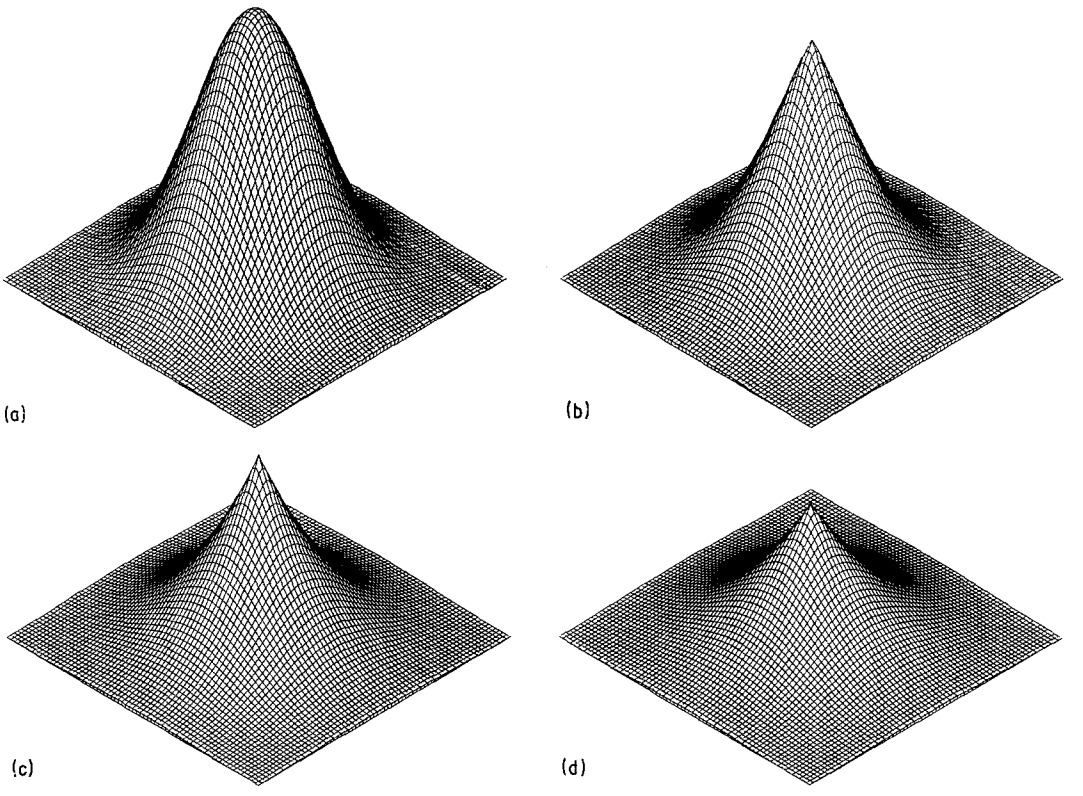

Figure 4 Three-dimensional simulations of an exponential hummock for a normal incidence ion beam, and for equally spaced timesteps. (a) $\phi t/N = 0$, (b) $\phi t/N = 0.2$ (c) $\phi t/N = 0.4$ and (d) $\phi t/N = 0.6$.

fixed half angle α, round the z-axis, with one rotation per $1/\beta$ sec. The following simulations were all carried out using the same scaling on the x, y and z axes, and equal timesteps. As a reference Figs. 4a–d illustrate the procedure for $\alpha = 0$, $\beta = 0$, i.e. a normal incidence ion beam. The development of a sharp cone from an initially smooth surface is clearly shown. The other noticeable feature is that the height of the cone decays with time, and the equilibrium situation arising after a long irradiation using this model would be a flat plane. Figs. 5a, b and c are simulations made with $\alpha = \pi/9$ and $\beta = 1$. The main feature to observe is that cone development is not supressed, and it is shown how features tend to follow the direction of the ion beam, causing bent cones. Figs. 6a b and c, then illustrate the technique for $\alpha = 2\pi/9$, $\beta = 1$. The rotation rate remaining constant, but the maximum angle α increased. A similar development of surface features is observed, and cone formation does not seem to be suppressed. Finally Figs. 7a, b and c show simulations for $\alpha = 2\pi/9$, and $\beta = 10$. The points to notice from these simulations are that cone development is suppressed by this choice of parameters, and also the eroded profiles seem to retain the initial surface features, thus appearing to preserve surface shape. Some slight tilting of the shape can be noticed, but due to the high rotation rate this is minimal. The conclusions that can be gathered from these simulations are:

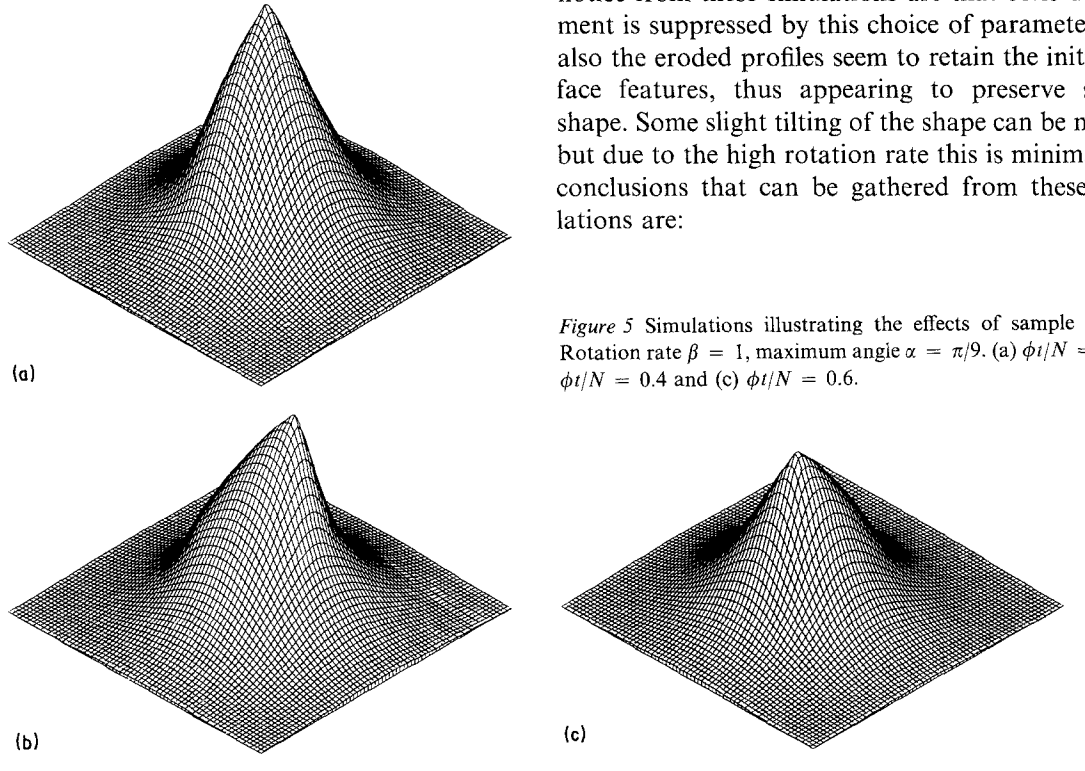

Figure 5 Simulations illustrating the effects of sample rotation. Rotation rate $\beta = 1$, maximum angle $\alpha = \pi/9$. (a) $\phi t/N = 0.2$, (b) $\phi t/N = 0.4$ and (c) $\phi t/N = 0.6$.

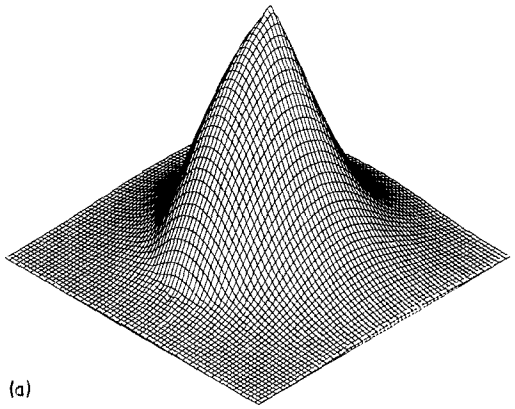

(a)

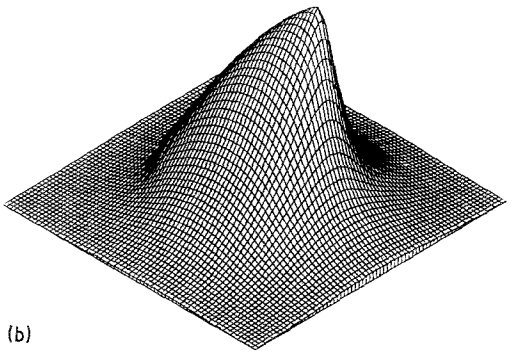

(b)

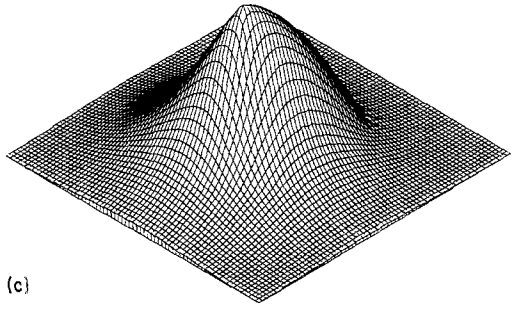

(c)

Figure 6 Simulations illustrating effects of sample rotation with increased maximum angle. Rotation rate $\beta = 1$, maximum angle $\alpha = 2\pi/9$. (a) $\phi t/N = 0.2$ (b) $\phi t/N = 0.4$ and (c) $\phi t/N = 0.6$.

1. Slow rotation rates at both low and high maximum angles will cause features which bend towards the direction of the ion beams.

2. High rotation rates and a large maximum angle optimize the preservation of surface shape and also suppress cone development.

6. Conclusion

This paper has given a theoretical treatment for the erosion of surfaces during ion bombardment, when the sample may be rocked and rotated. Experimental evidence is produced to provide details of how sample rotation affects surface topography. Computer simulations then show how initial topography is modified by varying rocking and rotation rates for some model initial surface profiles. By choosing large rocking and rotation rates compared with the erosion rate the initial surface topography can be preserved by averaging out angle of incidence effects and the formation of cones and pyramids can be suppressed. Comparisons made with the two-dimensional simulations produced by the two ion gun analysis [3] show that rocking and rotation can provide a greater flexibility over the final surface profile.

Acknowledgements

One of the authors, M. A. Tagg is grateful to the SERC and to the GEC for a studentship during the tenure of which this work was undertaken. We would like to thank the Hirst Research Centre and in particular Dr R. C. Peach for useful discussions and experimental facilities.

References

1. G. CARTER, B. NAVINSEK and J. L. WHITTON, in "Sputtering by Particle Bombardment II" edited by R. Behrisch (Springer Verlag, Berlin, 1983) p. 231.
2. D. E. SYKES, D. D. HALL, R. E. THURSTANS and J. M. WALLS, *Appl. Surf. Sci.* **5** (1980) 103.
3. S. S. MAKH, R. SMITH and J. M. WALLS, *J. Mater. Sci.* **17** (1982) 1689.
4. J. L. WHITTON, G. CARTER, M. J. NOBES and J. S. WILLIAMS, *Rad. Effects* **32** (1977) 129.

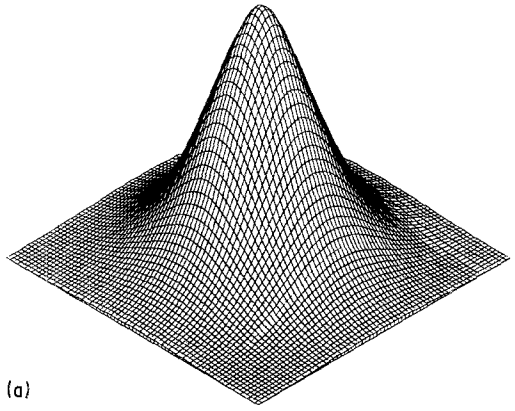

(a)

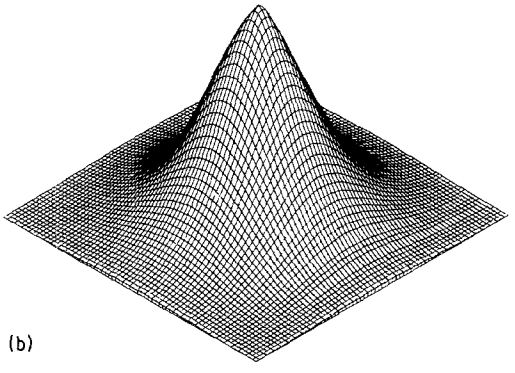

(b)

Figure 7 Simulations illustrating the effects of sample rotation with increased rotation rate. Rotation rate $\beta = 10$, maximum angle $\alpha = 2\pi/9$. (a) $\phi t/N = 0.2$ (b) $\phi t/N = 0.4$ and (c) $\phi t/N = 0.6$.

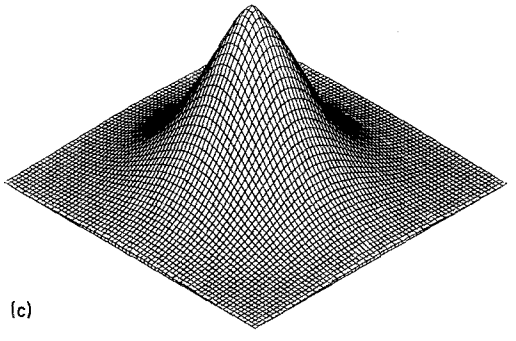

(c)

5. R. S. GVOSDOVER, V. M. EFREMENKOVA, L. B. SHELYAKIN and V. E. YURASOVA, *ibid.* **27** (1976) 237.
6. O. AUCIELLO and R. KELLY, *ibid.* **66** (1982) 195.
7. *Idem*, *ibid.* **46** (1980) 105.
8. R. CONG-XIN, C. GUO-MING, F. XIN-DING, Y. JIE, F. HONG-LI, and T. SHIH-CHANG, *ibid.* **77** (1983) 177.
9. G. CARTER, J. S. COLLIGON and M. J. NOBES, *ibid.* **31** (1977) 65.
10. A. D. G. STEWART and M. W. THOMPSON, *J. Mater. Sci.* **4** (1969) 56.
11. D. J. BARBER, F. C. FRANK, M. MOSS, J. W. STEEDS and I. S. T TSONG, *ibid.* **8** (1973) 1030.
12. G. CARTER, J. S. COLLIGON and M. J. NOBES, *ibid.* **8** (1973) 1473.
13. R. SMITH and J. M. WALLS, *Phil. Mag. A* **42**(2) (1980) 235.
14. R. SMITH, M. A. TAGG and J. M. WALLS, *Vacuum* **34** (1/2) (1984) 175.
15. R. SMITH, S. S. MAKH and J. M. WALLS, *Phil. Mag. A* **47**(4) (1983) 453.
16. A. R. NEUREUTHER, C. Y. LIU and C. H. TING, *J. Vac. Sci. Technol.* **16**(6) (1979) 1767.
17. G. CARTER, M. J. NOBES and S. A. CRUZ, *J. Mater. Sci. Lett.* **3** (1984) 523.
18. G. B. WHITHAM, "Linear and Non-Linear Waves" (Wiley, New York, 1974) 65.
19. C. F. GERALD, "Applied Numerical Analysis" (Addison Wesley, Reading, Massachusetts, 1977) Ch. 5.

Received 28 December 1984
and accepted 28 February 1985